Published in final edited form as:
Circ Res. 2012 August 3; 111(4): . doi:10.1161/CIRCRESAHA.112.269316.

Semaphorin3A, Neuropilin-1, and PlexinA1 Are Required for Lymphatic Valve Formation

Karine Bouvrée[*], **Isabelle Brunet**[*], **Raquel del Toro**, **Emma Gordon**, **Claudia Prahst**, **Brunella Cristofaro**, **Thomas Mathivet**, **Yunling Xu**, **Jihane Soueid**, **Vitor Fortuna**, **Nayoki Miura**, **Marie-Stéphane Aigrot**, **Charlotte H. Maden**, **Christiana Ruhrberg**, **Jean Léon Thomas**, and **Anne Eichmann**

CIRB Collège de France/CNRS UMR 7241/INSERM U1050, Paris, France (K.B., I.B., R.d.T., B.C., T.M., Y.X., V.F., A.E.); the Department of Cardiology, Yale University School of Medicine, New Haven, CT (E.G., C.P., A.E.); Inserm UMR-S 975, CNRS UMR 7225, UPMC, Hôpital de la Pitié-Salpêtrière, Paris, France (J.S., M.-S.A., J.L.T.); the Department of Biochemistry, Hamamatsu University School of Medicine, Hamamatsu, Japan (N.M.); Institute of Ophthalmology, University College London, London, United Kingdom (C.H.M., C.R.); and the Department of Neurology, Yale University School of Medicine, New Haven, CT (J.L.T.)

Abstract

Rationale—The lymphatic vasculature plays a major role in fluid homeostasis, absorption of dietary lipids, and immune surveillance. Fluid transport depends on the presence of intraluminal valves within lymphatic collectors. Defective formation of lymphatic valves leads to lymphedema, a progressive and debilitating condition for which curative treatments are currently unavailable. How lymphatic valve formation is regulated remains largely unknown.

Objective—We investigated if the repulsive axon guidance molecule Semaphorin3A (Sema3A) plays a role in lymphatic valve formation.

Methods and Results—We show that Sema3A mRNA is expressed in lymphatic vessels and that Sema3A protein binds to lymphatic valves expressing the Neuropilin-1 (Nrp1) and PlexinA1 receptors. Using mouse knockout models, we show that Sema3A is selectively required for lymphatic valve formation, via interaction with Nrp1 and PlexinA1. Sema3a$^{-/-}$ mice exhibit defects in lymphatic valve formation, which are not due to abnormal lymphatic patterning or sprouting, and mice carrying a mutation in the Sema3A binding site of Nrp1, or deficient for Plxna1, develop lymphatic valve defects similar to those seen in Sema3a$^{-/-}$ mice.

Conclusions—Our data demonstrate an essential direct function of Sema3A-Nrp1-PlexinA1 signaling in lymphatic valve formation.

Keywords

valve; guidance; development; lymphatic vessel; vascular biology; vascular smooth muscle

Correspondence to: Anne Eichmann, PhD, Department of Cardiology, Yale University School of Medicine, 300 George St, New Haven, CT 06510-3221. anne.eichmann@yale.edu.
[*]These authors contributed equally to this work.

The online-only Data Supplement is available with this article at http://circres.ahajournals.org/lookup/suppl/doi:10.1161/CIRCRESAHA.112.269316/-/DC1.

Disclosures
None.

The vertebrate circulatory system distributes oxygen, nutrients, and hormones to tissues and collects carbon dioxide and other metabolic waste products. Blood pressure causes plasma constituents to extravasate from the arterial side of the capillary bed into the interstitial space. The lymphatic system participates in the reabsorbance of this fluid and drains it back into the venous circulation. In healthy adult humans, the lymphatic system returns approximately 1 to 2 L of interstitial fluid with 20 to 30 g of protein per liter to the venous circulation every day.[1] The lymphatic network also plays a key role in immune responses by serving as a conduit for extravasated leukocytes and activated antigen-presenting cells.[2–4]

Blind-ended lymphatic capillaries are functionally specialized to allow entry of fluid containing macromolecules and leukocytes, termed lymph. Lymphatic capillaries form a highly branched network that permeates all body tissues, with the exception of bone and the central nervous system. In the small intestine, lacteal lymphatic capillaries inside the intestinal villi absorb chylomicrons of dietary lipids released by intestinal epithelial cells. Collecting lymphatic vessels transport the lymph through a network of progressively larger conduits back into the venous circulation.[5]

Structural differences between lymphatic capillaries and collecting vessels allow for efficient fluid uptake and transport, respectively. Capillaries exhibit button-like junctions that are anchored to filaments in the extracellular matrix (ECM), which exert tension to keep the junctions opened and allow fluid entry. In contrast, collecting lymphatic vessels have zipper-like junctions, which avoid fluid leakage.[6] Collecting lymphatics also develop valves, which prevent back-flow of lymph. Defects in valve formation cause congenital lymphedema, a severe and progressive condition characterized by gross swelling of the extremities accompanied by fibrosis and susceptibility to infections.[7]

Cellular and molecular mechanisms regulating lymphatic valve formation are only beginning to be understood. Valve formation in mice is initiated during late embryonic development by specification of valve forming cells, which are defined by high expression levels of the transcription factors Prox1 and Foxc2.[8] The same transcriptional program also regulates formation of venous valves[9] and is triggered by oscillatory shear stress in lymphatic valves, which often form at branch points of lymphatic vessels.[10] Foxc2 regulates positioning and specification of lymphatic valves within the collecting lymphatic vessels, and loss of Foxc2 leads to loss of luminal valves and abnormal lymph flow.[11] Mutations in human FOXC2 cause lymphedema-distichiasis.[12] After specification, lymphatic valve cells delaminate from the vessel wall, extend, and migrate into the lumen and mature into heart-shaped leaflets capable of preventing lymph back-flow.[10] The elongation process requires Integrin-α9 (Itgα9) interactions with fibronectin-EIIIA in the ECM.[13] Whether guidance molecules participate to lymphatic valve formation has not been investigated yet.

Sema3A, a member of class 3 secreted semaphorins, is expressed in adult lymphatic vessels and regulates entry of dendritic cells into lymphatics via an interaction with PlexinA1 and Neuropilin-1 (Nrp1) receptors expressed in dendritic cells.[4] Expression of Sema3A in lymphatic vessels suggested that Sema3A might play a role in lymphatic vessel development. We therefore investigated Sema3A expression in lymphatics and vascular development in *Sema3a*$^{-/-}$ mice. We show that Sema3A is expressed in neonatal lymphatic vessels and selectively regulates lymphatic valve formation but not sprouting or assembly of lymphatic vessels.

Sema3A binds to Nrp1, but in some cell types it has been shown to signal via the Neuropilin-2 (Nrp2) receptor.[14] Previous results demonstrated that Nrp2 is the predominant neuropilin expressed in lymphatic vessels, whereas Nrp1 is expressed in embryonic arteries.[15–19] We observed that expression of the Nrp1 receptor is elevated in lymphatic

valves and that Sema3A protein strongly binds to lymphatic valves. In contrast, Nrp2 expression is excluded from the lymphatic valve-forming area. In agreement with this expression pattern, *Nrp2* mutants formed normal lymphatic valves, whereas mice lacking *Sema3a* or carrying a mutation in the Sema3A binding site of Nrp1 (*Nrp1*$^{sema-/-}$,[20]) have small valves that were abnormally covered by smooth muscle cells (SMC). Furthermore, lymphatic valves express 1 of the 4 Plexin type A signal-transducing receptors, PlexinA1, and *Plxna1* mutants also have similar lymphatic valve defects. These results reveal a previously unanticipated and selective role for Sema3A-Nrp1-PlexinA1 signaling in the lymphatic component of the vascular system.

Results

To investigate Sema3A function in lymphatic vessel development, we first confirmed Sema3A expression in developing lymphatic vessels using in situ hybridization. Whole-mount staining of mesenteries from newborn mice showed robust labeling of lymphatic vessels but not arteries or veins with a *Sema3a* antisense riboprobe (Figure 1A). Sense probes did not show any signal (data not shown). To localize binding sites for Sema3A protein, we incubated mesenteries with an alkaline-phosphatase (AP)-tagged Sema3A protein (Sema3A-AP). Sema3A-AP bound prominently to lymphatic valves (Figure 1B). In contrast, AP-tagged VEGF-A protein bound to arteries and veins but not to lymphatic vessels (Figure 1C). This observation raised the possibility that Sema3A bound to cognate receptors on lymphatic valves to regulate valve formation.

Sema3A is known to bind to Nrp1 but can, in some cell types, also signal via Nrp2.[14] In situ hybridization showed that *Nrp1* mRNA was most prominently expressed in the lymphatic valve-forming areas (Figure 1D). Furthermore, lymphatic valve-forming areas expressed the Nrp1 coreceptor *Plxna1* (Figure 1E) but none of the other A-type plexins (Online Figure I). In contrast to *Nrp1* and *Plxna1*, *Nrp2* was expressed all along the mesenteric lymphatic vessels, but it appeared to be excluded from valve-forming areas (Figure 1F).[10] These observations suggested that lymphatic Sema3A might regulate valve formation through Nrp1-PlexinA1 signaling. In agreement with this hypothesis, Western blot analysis of cultured primary human dermal lymphatic endothelial cells (HDLEC) showed that these cells express Sema3A, Nrp1, and PlexinA1 protein (Figure 1G). Immunoprecipitation of HDLEC protein extracts with an anti-Nrp1 antibody pulled down PlexinA1 and Sema3A and pretreatment of HDLEC with Sema3A enhanced complex formation (Figure 1H).

If Sema3A signaled via Nrp1 and PlexinA1 to regulate development of lymphatic valves, mouse mutants for each of these signaling components might exhibit defects in valve formation. We analyzed the developing lymphatic vasculature of neonatal *Sema3a*$^{-/-}$ mice by staining with Foxc2 and Itgα9, 2 markers for lymphatic valve cells.[8] Mesenteric lymphatic valves in wild-type mice and in *Sema3a*$^{-/-}$ mutants both expressed Itgα9 and Foxc2 (Figure 2A through 2C), indicating that valves were properly specified in the absence of Sema3A. However, valve area was significantly smaller in *Sema3a*$^{-/-}$ mice when compared with wild-type littermates (Figure 2A, 2C, and 2E), suggesting that lack of Sema3A signaling impaired valve morphogenesis.

We next compared valve formation in mouse mutants deficient for *Nrp1*, *Plxna1*, or *Nrp2*. Because *Nrp1* null mutants die during early embryonic development,[18,21] we examined valve formation in mice carrying a deletion of the Sema3A binding site in the *Nrp1* gene.[20] These mice show normal vascular development, indicating that semaphorin binding to Nrp1 is dispensable for vascular development.[20,22] Strikingly, *Nrp1*$^{sema-/-}$ mice formed abnormally small lymphatic valves similar to those seen in *Sema3a*$^{-/-}$ mice (Figure 2D and 2E). Mice deficient in *Plxna1*[23] also developed smaller lymphatic valves (Figure 2E and

2F). Quantification of the diameter of lymphatic, arterial, and venous vessels showed no significant differences between wild-type and mutant littermates (see Methods), indicating that Sema3A, Nrp1, and PlexinA1 are required in the vasculature for proper morphogenesis of the lymphatic valves. In contrast, mesenteric lymphatic vessels and valves were of normal appearance in *Nrp2* knockout mice, and quantification of Itgα9-positive valve area showed no difference between wild-type and *Nrp2*$^{-/-}$ (Online Figure II), ruling out Nrp2 as a Sema3A receptor on valves.

We next asked if Sema3A signaling was selectively required in the developing vasculature for lymphatic valve formation or if the absence of Sema3A might impair other aspects of vascular or lymphatic vessel development.[22,24] To distinguish between these possibilities, we compared sprouting and assembly of lymphatic and blood vessels in wild-type and *Sema3a*$^{-/-}$ mice. High-magnification confocal analysis of lymphatic vessel sprouts showed a similar morphology in both genotypes and robust Nrp2 expression on sprouting tips (Figure 3A and 3B). We then intercrossed *Sema3a*$^{-/-}$ mice with a *Vegfr3::YFP* (yellow fluorescent protein) reporter mouse[25] to perform real-time monitoring of lymphatic vessel sprouting in the skin of newborn mice. Fluorescent images taken every 24 hours in the same pups showed that both wild-type and *Sema3a*$^{-/-}$ mice developed lymphatic sprouts that progressively covered the skin in the vicinity of the eyelid and that their overall length and number of branch points was similar in both genotypes (Figure 3C through 3F). These results show that lymphatic sprouting *Sema3a*$^{-/-}$ mice proceeds normally.

To investigate blood vascular patterning, we stained the skin of neonatal *Sema3a*$^{-/-}$ mutants and their littermates with the pan-endothelial marker CD31. Vascular development in the skin was similar between both genotypes (Online Figure III), consistent with previous results on embryonic vascular development in *Sema3a*$^{-/-}$ mutants.[22]

Finally, Sema3A is required for the normal fasciculation of peripheral nerve fibers,[26] which produce VEGF-A to induce arterial differentiation in the skin; consequently arteries follow disorganized nerve fibers in *Sema3a*$^{-/-}$ mice.[16,17] We considered that impaired sensory nerve and arterial patterning in *Sema3a*$^{-/-}$ mice might affect lymphatic vessel assembly and patterning. To address this possibility, we first compared the development of lymphatics, arteries, and sensory nerve fibers using confocal microscopy of whole-mount wild-type skin immunolabeled with specific markers (Figure 4A through 4D). We observed an alignment of large, future collecting Nrp2-positive lymphatics[15] with large Connexin40-positive (Cx40) arteries (Figure 4A and 4B). In contrast, smaller-diameter lymphatic vessel branches showed no alignment with smaller-diameter arterial branches, indicating that the coalignment of lymphatics and arteries is restricted to the large-vessel segments (Figure 4A and 4B). Sensory nerve fibers only aligned with smaller-diameter arterial branches and were neither aligned with the major arteries nor with the lymphatic vessels (Figure 4B through 4D).

We next compared the development of collecting lymphatic vessels in *Sema3a*$^{-/-}$ mice and their wild-type litter-mates intercrossed with the *Vegfr3::YFP* reporter mouse.[25] We observed that the large collecting lymphatics were positioned normally alongside major Nrp1-expressing arteries and that the patterning of both major arteries and collecting lymphatics was similar in both genotypes (Figure 4E through 4L). As lymphatic vessel patterning was initially normal in *Sema3a*$^{-/-}$ mice, valve defects seen in these mice at later stages cannot be secondary due to abnormal arterial patterning or branching of peripheral sensory axons. Given the absence of any detectable defects in angiogenesis or lymphatic vessel development besides the abnormal valves, we conclude that Sema3A is selectively required for lymphatic valve morphogenesis, in line with its strong binding to lymphatic valves.

Defective valve morphogenesis is expected to lead to aberrant lymph fluid transport.[7] However, detailed analysis of lymph fluid transport in *Sema3a*$^{-/-}$, *Nrp1*$^{sema-/-}$, or *Plxna1* mutants was impossible because of perinatal lethality of these mice.[20,23,27] Fluorescent dextran injection into the forelimb footpad of wild-type mice at postnatal day 6 (P6) showed that fluorescein isothiocyanate (FITC) is taken up by lymphatic capillaries and transferred to the axillary lymph nodes through one major unbranched collecting lymphatic[28] (Online Figure IV). In contrast, *Sema3a*$^{-/-}$ mice surviving until P6 displayed an increased area of FITC-perfused lymphatic vessels (Online Figure IV). Rhodamine-dextran into the footpad of P6 *Sema3a*$^{-/-}$ mice carrying a *Vegfr3::YFP* reporter showed small lymphatic valves located at branch points in the mutant collecting lymphatics that were insufficient to prevent backflow of the lymph into the side branch (Online Figure IV), suggesting that defective valve formation in *Sema3a* mutant mice may cause aberrant lymph drainage.

In addition to a reduction in valve size (Figure 2), *Sema3a*$^{-/-}$ mice exhibited abnormal SMC coating of the valve regions (Figure 5A through 5D). Thus, wild-type mice showed anti–smooth muscle actin (SMA)-positive staining of collecting mesenteric lymphatics, but valve-forming areas were devoid of SMC (Figure 5A and 5B). In contrast, the valve-forming areas of *Sema3a* mutant mice exhibited abnormal SMC coating (Figure 5C and 5D). Injecting neonatal mice with an antibody that blocks Sema3A binding to Nrp1 (anti-Nrp1^{A},[29]) also resulted in abnormal SMC coverage of valve areas (Figure 5E and 5F), whereas injection of an antibody that blocks VEGF binding to Nrp1 (anti-Nrp1^{B}) had no effect on SMC coverage (Figure 5G and 5H). We quantified the Itgα9-positive valve area covered by SMA-positive cells and found that it was significantly increased in *Sema3a*$^{-/-}$ and anti-Nrp1^{A}–treated mesenteries compared with controls (Figure 5I). These results suggest that in addition to valve-forming endothelial cells, Sema3A might act on SMC and repel them away from the valve-forming area.

Discussion

The results described here show that Sema3A is required for proper morphogenesis of lymphatic valves. Our study was prompted by the observation that Sema3A is expressed at high levels in adult lymphatic vessels.[4] Transcriptomic profiling of purified lymphatic endothelial cells (LECs) has confirmed that Sema3A expression is highly specific for LECs (M. Detmar, personal communication, 2008). We demonstrate expression of Sema3A mRNA in neonatal lymphatic vessels but not arteries or veins. Moreover, we found that Sema3A protein binds to lymphatic valves and that its receptors Nrp1 and PlexinA1 are strongly expressed by valve cells.

In line with its preferential binding to valves, our data show that Sema3A plays a selective role in lymphatic valve formation and that other aspects of vascular and lymphatic development including angiogenesis, lymphatic sprouting, and assembly proceed normally in the absence of Sema3A. We confirm previous reports of abnormal sensory nerve and arterial patterning in *Sema3a* mutants[17] and show that these defects do not affect lymphatic sprouting or assembly. Our data also confirm previous studies showing that Sema3A function is not required for developmental angiogenesis[22] except in certain vascular beds such as the kidney.[24,30] In contrast to developing vessels, systemic and targeted delivery of Sema3A has been shown to inhibit tumor angiogenesis,[31,32] indicating that Sema3A signaling is context dependent and regulated differently in developing and tumor vessels.

Nrp1 has previously been shown to be a direct Foxc2 target.[8] It is thus likely that Foxc2 activation leads to specification of future valve cells in the lymphatic wall and concomitant upregulation of Nrp1 expression in these cells. Our analysis of *Sema3a*$^{-/-}$, *Nrp1*$^{sema3a-/-}$, and *Plxna1*$^{-/-}$ mice shows that Foxc2 and Itgα9 are expressed in mutant valve cells. These

results suggest that valve cell become properly specified in the mutants and indicate that Sema3A-Nrp1 signaling functions downstream of the valve specification program to direct proper valve morphogenesis.

Our data support a dual role for Sema3A signaling in lymphatic valve formation. One possible mode for Sema3A-Nrp1-PlexinA1 signaling is that Sema3A, produced by the LEC wall, acts on Nrp1-PlexinA1– expressing cells in the newly specified valve to regulate their migration, perhaps generating a repulsive signal that “pushes” the valve cells away from the lymphatic wall to enable valve morphogenesis. Accordingly, the absence of Sema3A-Nrp1-PlexinA1 signaling leads smaller mesenteric valves (Figure 2), perhaps due to defective migration of valve-forming cells. Analysis of endothelial-specific *Nrp1* mutants will confirm if reduced valve size is due to lack of Sema3A signaling through Nrp1 in endothelial cells. In addition to their reduced size, valves in *Sema3a* mutants and in mice treated with an antibody blocking Sema3A binding to Nrp1 show increased SMC coverage (Figure 5), suggesting that Sema3A may repel SMC away from lymphatic valves. This could occur directly via receptor expression on SMC or indirectly via molecules secreted from receptor expressing valve cells. Our expression data show that valve cells preferentially produce Nrp1 and PlexinA1 mRNA and that Sema3A-AP strongly binds to valves. However, we cannot exclude that SMC surrounding lymphatics may express lower levels of Sema3A receptors, and arterial SMC lining the lymphatics express Nrp1.[33] Cultured vascular SMC express Sema3A, Nrp1, and PlexinA1 protein, and Sema3A and PlexinA1 can be coimmunoprecipitated with an antibody against Nrp1 in SMC and in HDLEC (Figure 1 and data not shown). SMC-specific deletion of Nrp1 will be required to determine if Sema3A signals through Nrp1 in SMC to repel them away from valve-forming areas.

Abnormal SMC coverage of lymphatic valves and loss of valve leaflets are also seen in mouse mutants for the transcription factor *Foxc2*[8,10,11] and contribute to lymphedema distichiasis in human patients with Foxc2 mutations,[12] highlighting the importance of coordinated extension of valve leaflet endothelial cells and repulsion of SMC from the lymph vessel wall. Future studies will determine if lack of Sema3A signaling in mice and in human patients may contribute to lymphedema formation.

Surprisingly, despite its prominent expression in the lymphatic system, *Nrp2* expression is excluded from lymphatic valves, and *Nrp2*-deficient mice show no defects in lymphatic valve formation. Lymphatic sprouts strongly express the Nrp2 receptor, and we have previously shown that LEC sprouting requires VEGF-C binding to a VEGFR3-Nrp2 complex.[19] Site-specific expression of guidance receptors could contribute to specific cell behaviors, and combinations of a repertoire of such receptors could possibly generate a multitude of different cell behaviors. There is precedence for the combinatorial use of neuropilin receptors in the literature. For example, Sema3A exerts a repulsive response on the axons of the facial motor nerve via Nrp1.[26] At the same time, Nrp1 is also expressed on the cell bodies of these neurons and binds VEGF, which guides their movement and is required for proper localization of the cell bodies within the hindbrain.[34] The same cell can therefore use different Nrp1 ligands to regulate movement at its front and rear end. Similarly, association of PlexinD1 with VEGFR2 regulates fasciculation of one specific axonal tract in the forebrain, whereas PlexinD1 associates with neuropilin receptors in other axonal tracts.[35] Combinatorial association of signaling modules, including binding and signal-transducing receptors, may be required to generate diverse cell behaviors in the vascular and nervous systems from a limited number of components. Strikingly, Sema3A in the lymphatic system plays a dual role—to regulate valve formation and communication with dendritic cells[4]—and both processes require interaction with the Nrp1 and PlexinA1 receptors.

Methods

Whole mount in situ hybridization

Mesenteries from mice between E18.5 and P4 were removed, postfixed in 4% PFA overnight at 4°C and kept in 100% MeOH at −20°C until further use. Mesenteries were then progressively rehydrated and washed in PBST (PBS/0.1% Tween-20). Thereafter, the mesenteries were treated with 80 μg/ml proteinase K/PBST for 11 min and postfixed for 20 min in 4% HCHO/1% Glutaraldehyde. After washing in PBST, tissues were incubated with hybridization mix (50% Formamide, 1.3x SSC, 5 mM EDTA, 50 mg/ml Yeast RNA, 0.2% Tween-20, 100 mg/ml heparin, 10% CHAPS) for 1 h at 70°C and then overnight in hybridization mix containing the probe at 70°C. The following day, mesenteries were extensively washed with hybridization mix and MABT (100 mM maleic acid, 150 mM NaCl, 1% Tween-20, pH 7.5) and blocked for 2 h in MABT/2% Blocking reagent (Boehringer Mannheim, Mannheim, Germany)/20% goat serum. The mesenteries were then incubated overnight at room temperature with blocking buffer containing anti-DIG-AP antibody (Roche). Next, the mesenteries were washed in MABT for 48 hours, rinsed in fresh NTMT (100 mM NaCl, 100 mM Tris-HCl pH 9.5, 50 mM MgCl2, 10% Tween-20) and developed with NTMT/0,33mg/ml nitroblue tetrazolium (NBT), 0.05 mg/ml 5-bromo-4-chloro-3-indolyl-phosphate (BCIP) at 37°C. Images were acquired on an Olympus BX50 microscope using a 4x/0.16 NA or 20x/0.05 NA objective and captured using a Coolsnap camera through IPLab software version 3.2.4 (Scanalytics Inc., Rockville, MD, USA). Probes were described previously [1, 2].

Alkaline Phosphatase (AP) staining

AP staining was performed as described previously [3]. Briefly, AP-fusion protein was generated by transfecting HEK293 cells using Fugene 6 (Roche) with VEGF-A and Sema3A-AP tagged expression vectors [3]. After 16 h, the medium was replaced and then collected 48 h later, centrifuged at 3000 rpm and stored at −20°C until further use. For whole mount AP staining, mesenteries were prefixed in 4% PFA, isolated and postfixed for 2 min with ice-cold MeOH. Thereafter, mesenteries were washed with TBS, blocked with TBS/1% FCS for 1 h and incubated overnight with AP fusion supernatant. The following day, mesenteries were washed in TBS, fixed in 60% acetone/5% Formaldehyde/20 mM Hepes for 90 sec. AP activity was quenched at 65°C for 2 h, followed by visualization with NBT/BCIP in NTMT at room temperature. Images were acquired on an Olympus BX50 microscope using a 4x/0.16 NA or 20x/0.05 NA objective and captured using a Coolsnap camera through IPLab software version 3.2.4 (Scanalytics Inc., Rockville, MD, USA).

Cell culture, Western blotting and Immunoprecipitation

HDLEC (Promocell) were cultured in complete Endothelial Cell Growth Medium MV2 (Promocell). For Western blotting analysis, HDLEC (2×10^5) were seeded in 60mm diameter dishes and cultured for 24h at 37°C and 5%CO2. Cells were lysed in RIPA buffer (20 mM Tris pH 7.5, 60 mM NaCl, 1% Triton X-100, 0.5% deoxycholic acid, 0.1% sodium dodecyl sulfate, 10% glycerol, 25 mM b-glycerophosphate, 50 mM sodium fluoride, 2 mM sodium pyrophosphate, 1 mM sodium orthovanadate, and 1X protease inhibitor cocktail, Calbiochem). Twenty-five micrograms of total proteins were separated on sodium dodecyl sulfate polyacrylamide gel electrophoresis (Invitrogen) and transferred to nitrocellulose membrane (GE Healthcare). Membranes were blocked in TBS, 0.1% Tween 20, 5% bovine serum albumin (BSA) followed by incubation at 4°C overnight with primary antibodies diluted in blocking buffer: anti-PlexinA1, anti-Neuropilin1 and anti-Sema3A (0.5μg/ml, R&D Systems). Membranes were washed and incubated with peroxidase-conjugated secondary antibodies (1:2000; Pierce) in blocking buffer for 2 hr at room temperature (RT),

and proteins were visualized with enhanced chemoluminescence western blotting detection reagents (Pierce). Membranes were exposed using the Fujifilm LAS-3000 imaging system.

For immunoprecipitation assays, HDLEC were seeded in 100mm diameter dishes, and cultured for 24h at 37°C and 5%CO2. HDLEC were starved for 12h in ECBM2 2%FBS; followed by serum-free ECBM-2 for 6h and treated with 2μg/ml recombinant Sema3A (R&D Systems) for 15 minutes. Cells were lysed in NP40-sodium desoxycholate buffer (20 mM Tris pH 7.5, 150 mM NaCl, 0.1% sodium desoxycholate, 0.5% NP40, 10% glycerol, 1 mM b-glycerophosphate, 1 mM NaF, 2.5 mM Na pyrophosphate, 1 mM Na_3VO_4, and 1X protease inhibitor cocktail (Calbiochem). Five hundred micrograms of total proteins were immunoprecipitated using anti-Neuropilin1 antibody (2μg; R&D Systems) on G-Sepharose beads (GE Healthcare). Protein separation and immunoblotting were described above.

Mice

All animal experiments were approved by institutional animal care and use committee. *Sema3a*$^{-/-}$ mutant mice were described previously [4]. Genotyping was carried out using the following primers:

Forward primer: 5′-GGAAAGACAATGTGCCAAGACTG-3′

Reverse primer 1: 5′-GTTCTGCTCCCGGCTCTAAATCTC-3′

Reverse primer 2: 5′-GCAAAGAACAATGTGCCAAGACTG -3′,

Genotyping was performed using Ready-To-Go PCR beads (Amersham Pharmacia). The PCR protocol consisted of 94°C for 5 min, 30 cycles of 94°C for 30 sec, 61°C for 1 min 10 sec and 72°C for 1 min 50 sec, followed by 10 min at 72°C.

Nrp1$^{sema-/-}$ mice (Jax) were described previously [5]. Genotyping was carried out using the following primers:

Forward primer: 5′-AGGCCAATCAAAGTCCTGAAAGACAGTCCC-3′

Reverse primer2: 5′-AAACCCCCTCAATTGATGTTAACACAGCCC-3′

The PCR protocol was composed of 94°C for 5 min, 35 cycles of 94°C for 45 sec, 63°C for 45 sec and 72°C for 45 sec, followed by 7 min at 72°C.

Plxna1 mutant mice were genotyped with the following primers:

Wild Type

Forward primer: 5′-CCTGCAGATTGATGACGACTTCTGC-3′

Reverse primer: 5′-TCATGCAGACCCAGTCTCCCTGTCA-3′

KO

Forward primer: 5′-CCATTGCTCAGCGGTGCTGTCCATC-3′

Reverse primer: 5′-GCATGCCTGTGACACTTGGCTCACT-3′

The PCR protocol was composed of 94°C for 3 min, 35 cycles of 94°C for 20 sec, 63°C for 45 sec and 72°C for 1 min 20 sec, followed by 10 min at 72°C.

Vegfr3::YFP mice were described and genotyped by assessing tail GFP staining [6]. *Nrp2*$^{-/-}$ mutant mice were described and genotyped as reported previously [3, 7].

Immunohistochemistry

For whole mount staining, dissected tissues/embryos were fixed in 4% paraformaldehyde (PFA) for 2h on ice and blocked overnight in blocking buffer (PBS/0.5% blocking reagent [Perkin]/0.3% Triton-X100/0.2% BSA). Tissues/embryos were incubated overnight at 4°C with primary antibodies in blocking buffer (anti-CD31, [Pharmingen 1/100]; anti-TuJ1 [R&D 1/100], anti-Nrp1 [R&D, 1/50], anti-Nrp2 [R&D, 1/50], anti-Cx40 [Interchim, 1/100], anti-Integrin-α9 [R&D 1/100] and Cy3-conjugated anti-SMA [Sigma, 1/500]). Tissues/embryos were washed in PBS/0.3%TX-100 and incubated overnight with fluorescent streptavidin (Cy2 or Cy3, GE Healthcare), or species-specific fluorescent secondary antibodies (Alexa 488, 555 or 647, Invitrogen). The samples were then washed in PBS/0.3%TX-100 and mounted (Dako Fluorescent Mounting Medium, Dako). Images were captured using a confocal microscope (Sp5; Leica) with acquisition software (LAS AF; Leica) and a 103 NA 0.3 Plan Fluotar lens (HC; Leica), a 203 NA 0.7 Plan Apo lens (HCX CS; Leica), and a 403 NA 1.4 Plan Apo lens (HCX CS; Leica).

VEGFR3::YFP-*Sema3a*$^{-/-}$ sprout imaging

Pups were imaged at P0, P1, P2 and P3 at an identical location in the skin of the eyelid each day. Images were acquired using a fluorescent microscope (Leica MZFLIII FluoTM) using a Leica Plan Apo 1X objective and Metamorph software.

Quantification of valves, arterial, venous and lymphatic vessels

Itgα9-positive valve area was measured using 8–10 images from 3 mice of each genotype at P0. Valve area was quantified using ImageJ and expressed as percent of wildtype values. Lymphatic diameter was measured by tracing the perimeter of lymphatic vessels on images from mesentery wholemounts. Arterial and venous diameter was calculated as the average of five different measurements throughout the vessel length. Three to ten anti-CD31 stained images per mouse from three to four mice/genotype at P0 were analyzed using MetaMorph software. Values in mutants were expressed as percent of wildtype values (mean±SEM). Smooth muscle cell coverage was quantified using ImageJ from n>4 mice per genotype at P4 (*Sema3a*) or P5 (Nrp1^{A}- and Nrp1^{B}-antibody injected mice). Values are expressed as the percentage of SMA-positive immunostaining over the total valve area (as determined by Itgα9-positive immunostaining). Statistical significance was evaluated by using Mann-Whitney test.

Mutant mice did not show any significant difference in lymphatic vessel area compared to wild type littermates (1±0.057 in *Sema3a*$^{+/+}$ versus 0.775±0.059 in *Sema3a*$^{-/-}$ P=0.0513; 1±0.056 in *Plxna1*$^{+/+}$ versus 0.897±0.067 in *Plxna1*$^{-/-}$ P=0.3056; 1±0.136 in *Nrp1*-$^{Sema3a+/+}$ versus 1.051±0.039 in *Nrp1*-$^{Sema3a-/-}$ P=0.8333). Arterial and vein diameter was also similar between mice (arteries: 1±0.044 in *Sema3a*$^{+/+}$ versus 0.899±0.078 in *Sema3a*$^{-/-}$ P=0.2567, 1±0.088 in *Plxna1*$^{+/+}$ versus 0.996±0.0310 in *Plxna1*$^{-/-}$ P=0.4293; veins: 1±0.047 in *Sema3a*$^{+/+}$ versus 0.874±0.062 in *Sema3a*$^{-/-}$ P=0.2240; 1±0.058 in *Plxna1*$^{+/+}$ versus 1.168±0.181 in *Plxna1*$^{-/-}$ P=0.6785).

FITC-dextran injection in the mouse forelimb footpad

Mice were anesthetized by intraperitoneal injection of ketamine-xylazine (2:1 mix). Using a fine microliter syringe, approximately 3 μl of 5 mg/ml FITC-dextran (FITC: Fluorescein isothiocyanate–dextran; 2 000 000 MW; Sigma) was injected through the forelimb footpad. After one or two minutes, FITC is taken up by initial lymphatics and is transferred to axillary lymph nodes through collecting lymphatics. The skin near the forelimb was removed and images were taken under a fluorescent dissecting microscope (Leica MZFLIII FluoTM) using a Leica Plan Apo 0.63X objective, and captured using a camera (Coolsnap)

and Metamorph software (Roper Scientific). ImageJ software (http://rsb.info.nih.gov/ij/) was used to quantify the length of the FITC perfused collecting lymphatic vessels.

Neonatal mouse injections

At day P0, P1, P2 and P3, wild type pups on a CD1 background (n > 3 per group) received intraperitoneal injections with 10 mg/kg of anti-Nrp1A antibody, anti-Nrp1B antibody (Pan et al., 2007) or PBS. Neonatal pups were collected for analysis at day P5.

Supplementary Material

Refer to Web version on PubMed Central for supplementary material.

Acknowledgments

We thank Yutaka Yoshida and Thomas Jessell for the *Plxna1* mice, Genentech for the anti-Nrp antibodies, and Laura Denti for technical assistance.

Sources of Funding

This work was supported by grants from NIH (1R01HL111504-01), Inserm, Agence Nationale de la Recherche, Fondation pour la Recherche Médicale (FRM), Fondation Leducq (Artemis Transatlantic Network of Excellence), and Fondation Bettencourt. K.B. was supported by Association pour la Recherche contre le Cancer. I.B. was supported by Nerf. R.d.T. and B.C. were supported by FRM. E.G. was supported by a Brown-Coxe fellowship. C.P. was supported by Deutsche Forschungsgemeinschaft.

Non-standard Abbreviations and Acronyms

AP	alkaline phosphatase
ECM	extracellular matrix
FITC	fluorescein isothiocyanate
HDLEC	human dermal lymphatic endothelial cells
Itgα9	Integrin-α9
LEC	lymphatic endothelial cell
Nrp1	Neuropilin-1
P	postnatal day
Sema3A	Semaphorin3A
SMA	smooth muscle actin
SMC	smooth muscle cell(s)
YFP	yellow fluorescent protein

References

1. Foldi M. Remarks concerning the consensus document (CD) of the International Society of Lymphology: “The diagnosis and treatment of peripheral lymphedema”. Lymphology. 2004; 37:168–173. [PubMed: 15693529]
2. Kosco-Vilbois M, Meyer-Hermann M. The 16th International Conference on Lymphatic Tissues and Germinal Centers in Immune Responses. Eur J Immunol. 2009; 39:2311–2312. [PubMed: 19714570]
3. Sapin MR. Lymphatic system and its significance in immune processes. Morfologiia. 2007; 131:18–22. [PubMed: 17526257]

4. Takamatsu H, Takegahara N, Nakagawa Y, et al. Semaphorins guide the entry of dendritic cells into the lymphatics by activating myosin II. Nat Immunol. 2010; 11:594–600. [PubMed: 20512151]
5. Tammela T, Alitalo K. Lymphangiogenesis: molecular mechanisms and future promise. Cell. 2010; 140:460–476. [PubMed: 20178740]
6. Baluk P, Fuxe J, Hashizume H, Romano T, Lashnits E, Butz S, Vestweber D, Corada M, Molendini C, Dejana E, McDonald DM. Functionally specialized junctions between endothelial cells of lymphatic vessels. J Exp Med. 2007; 204:2349–2362. [PubMed: 17846148]
7. Rockson SG. Lymphedema. Am J Med. 2001; 110:288–295. [PubMed: 11239847]
8. Norrmén C, Ivanov KI, Cheng J, Zangger N, Delorenzi M, Jaquet M, Miura N, Puolakkainen P, Horsley V, Hu J, Augustin HG, Ylä-Herttuala S, Alitalo K, Petrova TV. FOXC2 controls formation and maturation of lymphatic collecting vessels through cooperation with NFATc1. J Cell Biol. 2009; 185:439–457. [PubMed: 19398761]
9. Bazigou E, Lyons OT, Smith A, Venn GE, Cope C, Brown NA, Makinen T. Genes regulating lymphangiogenesis control venous valve formation and maintenance in mice. J Clin Invest. 2011; 121:2984–2992. [PubMed: 21765212]
10. Sabine A, Agalarov Y, Maby-El Hajjami H, et al. Mechanotransduction, PROX1, and FOXC2 cooperate to control connexin37 and calcineurin during lymphatic-valve formation. Dev Cell. 2012; 22:430–445. [PubMed: 22306086]
11. Petrova TV, Karpanen T, Norrmén C, Mellor R, Tamakoshi T, Finegold D, Ferrell R, Kerjaschki D, Mortimer P, Ylä-Herttuala S, Miura N, Alitalo K. Defective valves and abnormal mural cell recruitment underlie lymphatic vascular failure in lymphedema distichiasis. Nat Med. 2004; 10:974–981. [PubMed: 15322537]
12. Fang J, Dagenais SL, Erickson RP, Arlt MF, Glynn MW, Gorski JL, Seaver LH, Glover TW. Mutations in FOXC2 (MFH-1), a forkhead family transcription factor, are responsible for the hereditary lymphedema-distichiasis syndrome. Am J Hum Genet. 2000; 67:1382–1388. [PubMed: 11078474]
13. Bazigou E, Xie S, Chen C, Weston A, Miura N, Sorokin L, Adams R, Muro AF, Sheppard D, Makinen T. Integrin-alpha9 is required for fibronectin matrix assembly during lymphatic valve morphogenesis. Dev Cell. 2009; 17:175–186. [PubMed: 19686679]
14. Cariboni A, Davidson K, Rakic S, Maggi R, Parnavelas JG, Ruhrberg C. Defective gonadotropin-releasing hormone neuron migration in mice lacking SEMA3A signalling through NRP1 and NRP2: implications for the aetiology of hypogonadotropic hypogonadism. Hum Mol Genet. 2010; 20:336–344. [PubMed: 21059704]
15. Yuan L, Moyon D, Pardanaud L, Bréant C, Karkkainen MJ, Alitalo K, Eichmann A. Abnormal lymphatic vessel development in neuropilin 2 mutant mice. Development. 2002; 129:4797–4806. [PubMed: 12361971]
16. Mukouyama Y-S, Gerber H-P, Ferrara N, Gu C, Anderson DJ. Peripheral nerve-derived VEGF promotes arterial differentiation via neuropilin 1-mediated positive feedback. Development. 2005; 132:941–952. [PubMed: 15673567]
17. Mukouyama, Y-s; Shin, D.; Britsch, S.; Taniguchi, M.; Anderson, DJ. Sensory nerves determine the pattern of arterial differentiation and blood vessel branching in the skin. Cell. 2002; 109:693–705. [PubMed: 12086669]
18. Jones EA, Yuan L, Breant C, Watts RJ, Eichmann A. Separating genetic and hemodynamic defects in neuropilin 1 knockout embryos. Development. 2008; 135:2479–2488. [PubMed: 18550715]
19. Xu Y, Yuan L, Mak J, Pardanaud L, Caunt M, Kasman I, Larrivee B, Del Toro R, Suchting S, Medvinsky A, Silva J, Yang J, Thomas J-L, Koch AW, Alitalo K, Eichmann A, Bagri A. Neuropilin-2 mediates VEGF-C-induced lymphatic sprouting together with VEGFR3. J Cell Biol. 2010; 188:115–130. [PubMed: 20065093]
20. Gu C, Rodriguez ER, Reimert DV, Shu T, Fritzsch B, Richards LJ, Kolodkin AL, Ginty DD. Neuropilin-1 conveys semaphorin and VEGF signaling during neural and cardiovascular development. Dev Cell. 2003; 5:45–57. [PubMed: 12852851]
21. Kawasaki T, Kitsukawa T, Bekku Y, Matsuda Y, Sanbo M, Yagi T, Fujisawa H. A requirement for neuropilin-1 in embryonic vessel formation. Development. 1999; 126:4895–4902. [PubMed: 10518505]

22. Vieira JM, Schwarz Q, Ruhrberg C. Selective requirements for NRP1 ligands during neurovascular patterning. Development. 2007; 134:1833–1843. [PubMed: 17428830]

23. Yoshida Y, Han B, Mendelsohn M, Jessell TM. PlexinA1 signaling directs the segregation of proprioceptive sensory axons in the developing spinal cord. Neuron. 2006; 52:775–788. [PubMed: 17145500]

24. Serini G, Valdembri D, Zanivan S, Morterra G, Burkhardt C, Caccavari F, Zammataro L, Primo L, Tamagnone L, Logan M, Tessier-Lavigne M, Taniguchi M, Püschel AW, Bussolino F. Class 3 semaphorins control vascular morphogenesis by inhibiting integrin function. Nature. 2003; 424:391–397. [PubMed: 12879061]

25. Calvo CF, Fontaine RH, Soueid J, et al. Vascular endothelial growth factor receptor 3 directly regulates murine neurogenesis. Genes Dev. 2011; 25:831–844. [PubMed: 21498572]

26. Kawasaki T, Bekku Y, Suto F, Kitsukawa T, Taniguchi M, Nagatsu I, Nagatsu T, Itoh K, Yagi T, Fujisawa H. Requirement of neuropilin 1-mediated Sema3A signals in patterning of the sympathetic nervous system. Development. 2002; 129:671–680. [PubMed: 11830568]

27. Taniguchi M, Yuasa S, Fujisawa H, Naruse I, Saga S, Mishina M, Yagi T. Disruption of semaphorin III/D gene causes severe abnormality in peripheral nerve projection. Neuron. 1997; 19:519–530. [PubMed: 9331345]

28. Tammela T, He Y, Lyytikkä J, Jeltsch M, Markkanen J, Pajusola K, Ylä-Herttuala S, Alitalo K. Distinct architecture of lymphatic vessels induced by chimeric vascular endothelial growth factor-C/vascular endothelial growth factor heparin-binding domain fusion proteins. Circ Res. 2007; 100:1468–1475. [PubMed: 17478733]

29. Pan Q, Chanthery Y, Liang W-C, et al. Blocking neuropilin-1 function has an additive effect with anti-VEGF to inhibit tumor growth. Cancer Cell. 2007; 11:53–67. [PubMed: 17222790]

30. Reidy KJ, Villegas G, Teichman J, Veron D, Shen W, Jimenez J, Thomas D, Tufro A. Semaphorin3a regulates endothelial cell number and podocyte differentiation during glomerular development. Development. 2009; 136:3979–3989. [PubMed: 19906865]

31. Casazza A, Fu X, Johansson I, Capparuccia L, Andersson F, Giustacchini A, Squadrito ML, Venneri MA, Mazzone M, Larsson E, Carmeliet P, De Palma M, Naldini L, Tamagnone L, Rolny C. Systemic and targeted delivery of semaphorin 3A inhibits tumor angiogenesis and progression in mouse tumor models. Arterioscler Thromb Vasc Biol. 2011; 31:741–749. [PubMed: 21205984]

32. Maione F, Molla F, Meda C, Latini R, Zentilin L, Giacca M, Seano G, Serini G, Bussolino F, Giraudo E. Semaphorin 3A is an endogenous angiogenesis inhibitor that blocks tumor growth and normalizes tumor vasculature in transgenic mouse models. J Clin Invest. 2009; 119:3356–3372. [PubMed: 19809158]

33. Pellet-Many C, Frankel P, Evans IM, Herzog B, Junemann-Ramirez M, Zachary IC. Neuropilin-1 mediates PDGF stimulation of vascular smooth muscle cell migration and signalling via p130Cas. Biochem J. 2011; 435:609–618. [PubMed: 21306301]

34. Schwarz Q, Gu C, Fujisawa H, Sabelko K, Gertsenstein M, Nagy A, Taniguchi M, Kolodkin AL, Ginty DD, Shima DT, Ruhrberg C. Vascular endothelial growth factor controls neuronal migration and cooperates with Sema3A to pattern distinct compartments of the facial nerve. Genes Dev. 2004; 18:2822–2834. [PubMed: 15545635]

35. Chauvet S, Cohen S, Yoshida Y, Fekrane L, Livet J, Gayet O, Segu L, Buhot M-C, Jessell TM, Henderson CE, Mann F. Gating of Sema3E/PlexinD1 signaling by neuropilin-1 switches axonal repulsion to attraction during brain development. Neuron. 2007; 56:807–822. [PubMed: 18054858]

Methods references

1. Moyon D, Pardanaud L, Yuan L, Bréant C, Eichmann A. Plasticity of endothelial cells during arterial-venous differentiation in the avian embryo. Development. 2001; 128:3359–3370. [PubMed: 11546752]

2. Schwarz Q, Vieira JM, Howard B, Eickholt BJ, Ruhrberg C. Neuropilin 1 and 2 control cranial gangliogenesis and axon guidance through neural crest cells. Development. 2008; 135:1605–1613. [PubMed: 18356247]

3. Xu Y, Yuan L, Mak J, Pardanaud L, Caunt M, Kasman I, Larrivee B, Del Toro R, Suchting S, Medvinsky A, Silva J, Yang J, Thomas J-L, Koch AW, Alitalo K, Eichmann A, Bagri A. Neuropilin-2 mediates VEGF-C-induced lymphatic sprouting together with VEGFR3. The Journal of Cell Biology. 2010; 188:115–130. [PubMed: 20065093]

4. Taniguchi M, Yuasa S, Fujisawa H, Naruse I, Saga S, Mishina M, Yagi T. Disruption of semaphorin III/D gene causes severe abnormality in peripheral nerve projection. Neuron. 1997; 19:519–530. [PubMed: 9331345]

5. Gu C, Rodriguez ER, Reimert DV, Shu T, Fritzsch B, Richards LJ, Kolodkin AL, Ginty DD. Neuropilin-1 conveys semaphorin and VEGF signaling during neural and cardiovascular development. Developmental Cell. 2003; 5:45–57. [PubMed: 12852851]

6. Calvo CF, Fontaine RH, Soueid J, Tammela T, Makinen T, Alfaro-Cervello C, Bonnaud F, Miguez A, Benhaim L, Xu Y, Barallobre MJ, Moutkine I, Lyytikka J, Tatlisumak T, Pytowski B, Zalc B, Richardson W, Kessaris N, Garcia-Verdugo JM, Alitalo K, Eichmann A, Thomas JL. Vascular endothelial growth factor receptor 3 directly regulates murine neurogenesis. Genes & Dev. 2011; 25:831–844. [PubMed: 21498572]

7. Giger RJ, Cloutier JF, Sahay A, Prinjha RK, Levengood DV, Moore SE, Pickering S, Simmons D, Rastan S, Walsh FS, Kolodkin AL, Ginty DD, Geppert M. Neuropilin-2 is required in vivo for selective axon guidance responses to secreted semaphorins. Neuron. 2000; 25:29–41. [PubMed: 10707970]

Novelty and Significance

What Is Known?

- The lymphatic vascular system plays an important role in the transport of interstitial fluid from tissues back to the bloodstream.
- To allow efficient fluid transport, collecting vessels contain a smooth muscle layer and intraluminal valves that prevent fluid backflow.
- The signals that guide valve formation and trigger delamination of valve cells from the lymphatic vessel wall to form a functional valve leaflet remain uncharacterized.

What New Information Does This Article Contribute?

- This study demonstrates the expression of Semaphorin3A, Neuropilin 1, and PlexinA1 in the lymphatic compartment of the vascular system.
- Mice defective for Semaphorin3A, Neuropilin 1, or PlexinA1 signaling have small lymphatic valves with abnormal smooth muscle cell coverage, which are insufficient to prevent backflow of the lymph into the side branches of collecting vessels.
- These results uncover guidance cues important for the morphogenesis of a functional valve leaflet.

Lymphatic vessels control fluid homeostasis by capturing extravasated fluid and transporting it back to the bloodstream. To allow efficient fluid transport, lymphatic vessels contain a smooth muscle layer and intraluminal valves that prevent fluid backflow. The signals important for lymphatic valve specification and assembly of the supporting fibrin matrix have been identified; however, the cues that guide the formation of a functional valve leaflet remain unknown. This study shows, for the first time, that the guidance molecule Semaphorin 3A can bind to Neuropilin 1 and PlexinA1 expressed in the valve-forming areas of the lymphatic endothelium. This interaction guides the migration of endothelial cells to form a functional valve leaflet, which promotes unidirectional flow of lymph back to the bloodstream. These results identify cues important for valve morphogenesis. Semaphorin 3A was not required for lymphatic vessel sprouting or branching; therefore these results reveal a previously unanticipated and selective role for Sema3A-Nrp1-PlexinA1 signaling in the lymphatic component of the vascular system. Because functional lymphatic valves are important in human disease such as primary lymphedema, these results may provide novel therapeutic targets for the treatment of this inherited, debilitating disease.

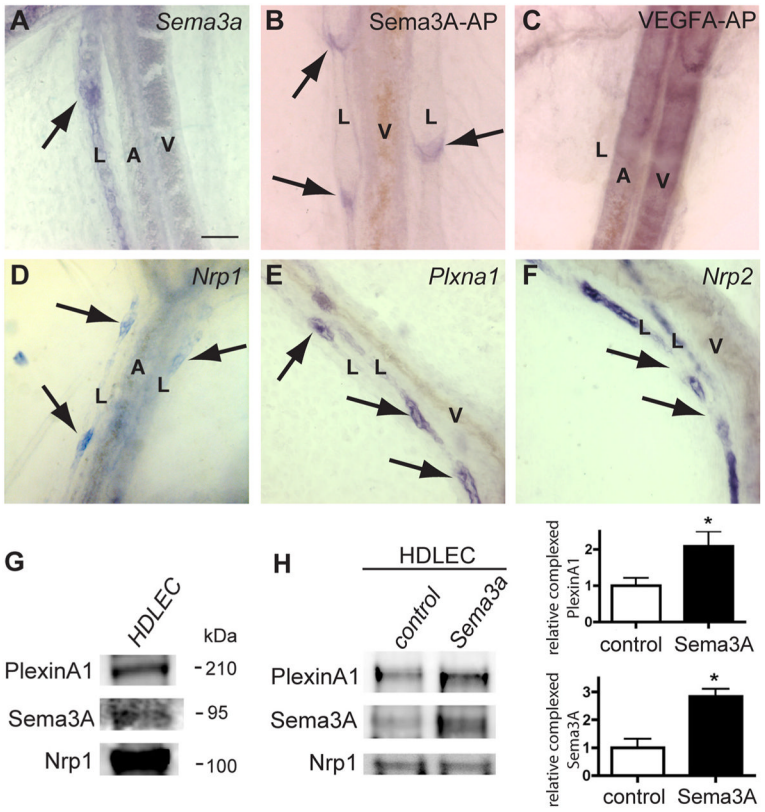

Figure 1. Sema3A expression and binding to lymphatic valves expressing Nrp1 and PlexinA1

A, In situ hybridization with *Sema3a* antisense riboprobe on P0 mesenteric vessels. Note specific labeling of lymphatic vessels (L) including valve-forming areas (**arrow**) but not arteries (A) or veins (V). **B** and **C**, Sema3A-AP (**B**) and VEGFA-AP (**C**) fusion protein binding to whole-mount mesenteries from wild-type mice at P0. Sema3A-AP binds to lymphatic valves (**B**, **arrows**). VEGFA-AP binds to arteries and veins but not to lymphatics (**C**). **D** through **F**, In situ hybridization of whole-mount mesenteries at P0 with the indicated antisense riboprobes. *Nrp1* and *Plxna1* label valve-forming areas of lymphatic vessels (**D** and **E**, **arrows**). Note strong *Nrp2* staining in lymphatic vessels but absence of signal in valve-forming areas (**arrows**, **F**). **G**, HDLEC protein extracts subjected to sodium dodecyl sulfate polyacrylamide gel electrophoresis and Western blots were incubated with the indicated antibodies. HDLEC express Nrp1, PlexinA1, and Sema3A. **H**, HDLEC were serum-starved and stimulated with Sema3A for 15 minutes. Nrp1 was immunoprecipitated from cultures, and Western blots were probed with indicated antibodies. Quantification of 3 independent experiments shows that Sema3A treatment enhances Nrp1/PlexinA1 complex formation. Bars represent SEM. **P*<0.05 (*t* test). Scale bars: 50 μm.

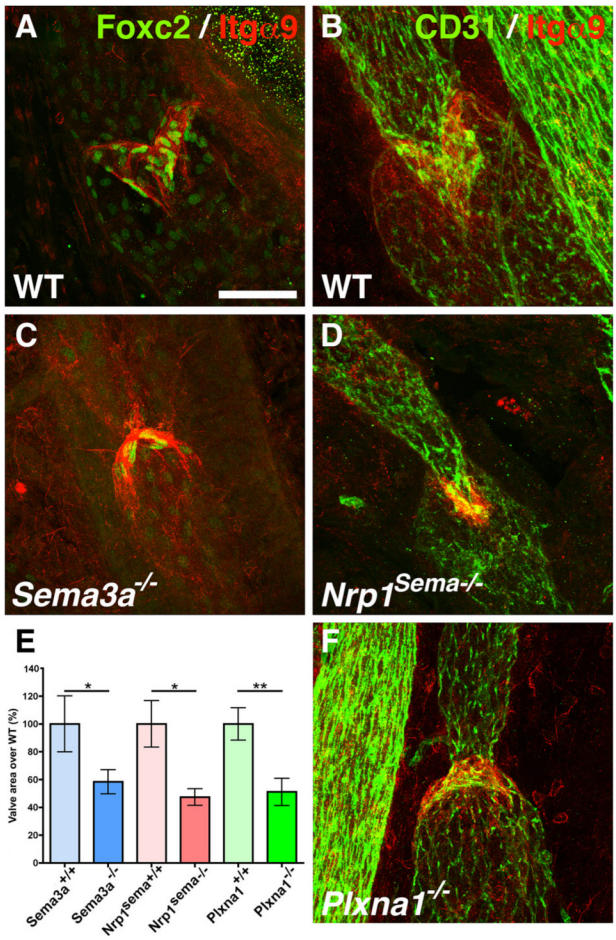

Figure 2. Abnormal lymphatic valves in *Sema3a*$^{-/-}$, *Nrp1*$^{sema-/-}$ and *Plxna1*$^{-/-}$ mice

Confocal images of whole-mount mesenteries stained with the indicated antibodies. **A** and **B**, Anti-Foxc2 (**A**, green) and anti-Itgα9 (**A** and **B**, red) staining in wild-type mesentery lymphatics show normal valve leaflets. **C**, **D**, and **F**, Staining of mutant mouse mesenteries with the indicated markers. Note abnormal valves in *Sema3a*$^{-/-}$ (**C**), *Nrp1*$^{sema-/-}$ (**D**), and *Plxna1*$^{-/-}$ (**F**) compared with wild-type (**A** and **B**). **E**, Itgα9-positive valve area was measured using 8 to 10 images from 3 mice of each genotype at P0. Note reduction of valve area in all 3 mutant mouse lines. Quantification was performed using ImageJ (Mann-Whitney *U* test, $P<0.05$). Scale bars: 90 μm.

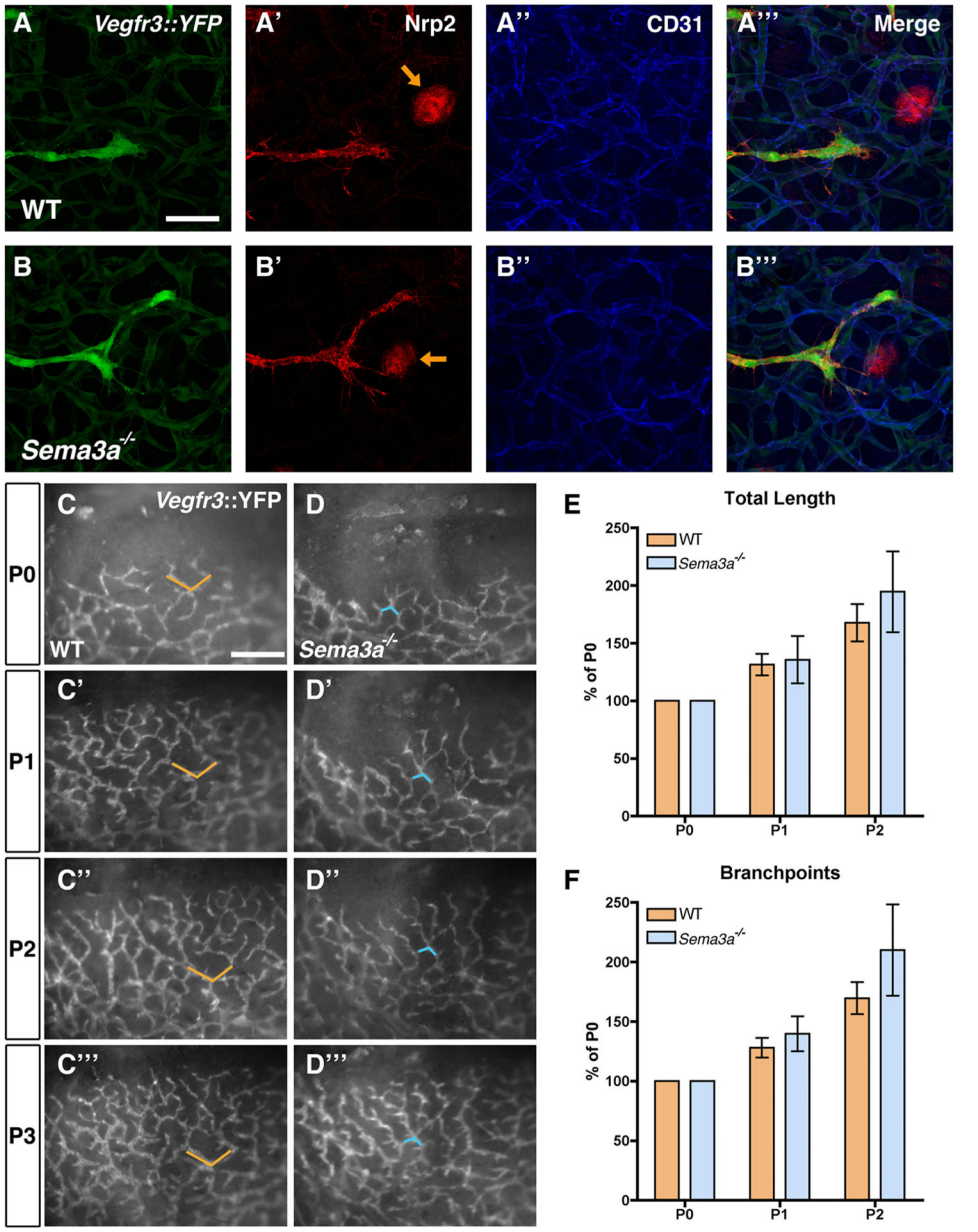

Figure 3. Normal lymphatic sprouting in *Sema3a*$^{-/-}$ mice

A through **B‴**, Confocal images of lymphatic sprouts in E14.5 skin from *Vegfr3::YFP, WT* (**A**) or *Vegfr3::YFP, Sema3a*$^{-/-}$ (**B**) embryos, labeled with Nrp2 (red), and anti-CD31 (blue). Note normal appearance of lymphatic sprouts in *WT* and in *Sema3a*$^{-/-}$ mice. Hair follicles: orange **arrows. C** and **D**, Live imaging of lymphatic vessel sprouting in *Vegfr3::YFP, WT* (**C** through **C‴**) and *Vegfr3::YFP, Sema3a*$^{-/-}$ (**D** through **D‴**) mice. Single images were captured every day in the same position in eyelid skin, between P0 and P3 in *Vegfr3::YFP, WT* mice (**C** through **C‴**) and in *Vegfr3::YFP, Sema3a*$^{-/-}$ mice (**D** through **D‴**). Orange and blue markers indicate the same position among the lymphatic capillaries. **E** and **F**, Quantification of total length (**E**) and number of branch points (**F**) of growing lymphatic capillaries from P0 to P2 in *Vegfr3::YFP, WT* and *Vegfr3::YFP, Sema3a*$^{-/-}$ mice. Note similar increase in length and branch point number in animals of both genotypes.

Quantification was performed using ImageJ ($P>0.05$); n=3 mice/genotype. Scale bars: 57 μm (**A** through **B‴**); 426 μm (**C** through **D‴**).

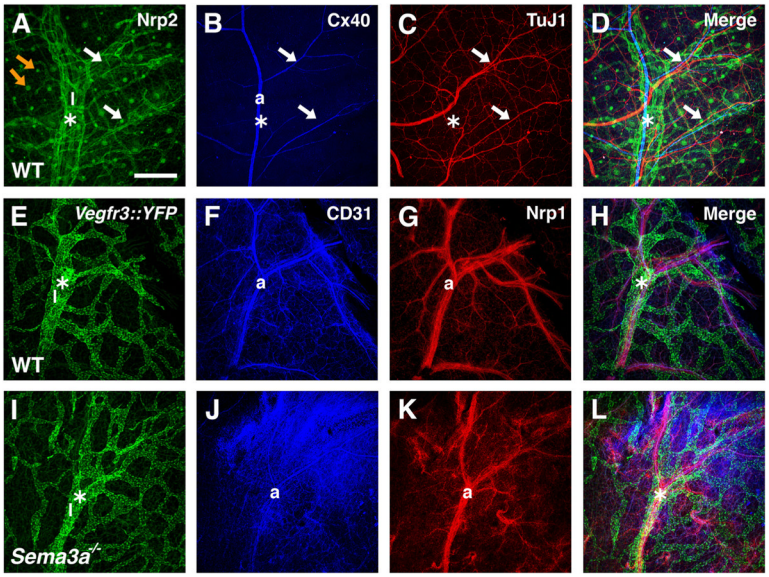

Figure 4. Development of sensory nerves, arteries, and lymphatics in *Sema3a*$^{-/-}$ mice

Confocal images of whole-mount skin from embryos at E15.5 (**E** through **L**) or E14.5 (**A** through **D**) stained with the indicated antibodies. **A** through **D**, In wild-type, Nrp2-positive collecting lymphatic vessels (labeled as **l*** in **A**) develop along the main branches of a Cx40-positive artery (labeled as **a** in **B**). Note Nrp2 expression in hair follicles (**orange arrows, A**). Only the small-diameter arteries are aligned with TuJ1-positive sensory axons (**arrows** in **B** through **D**). E through **L**, Normal development of collecting lymphatics (labeled as **l***) alongside main arterial Nrp1-positive branches in wild-type (**E** through **H**) and *Sema3a*$^{-/-}$ (**I** through **L**) mice. Lymphatics are labeled with a *Vegfr3::YFP* reporter. Scale bars: 208 μm.

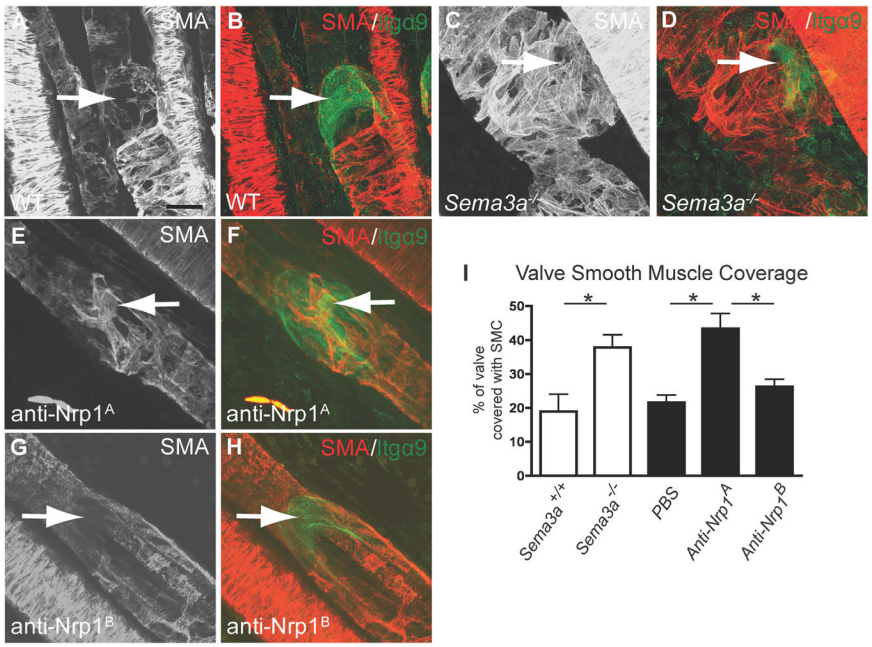

Figure 5. Abnormal smooth muscle coating in *Sema3a*$^{-/-}$ mice and mice treated with anti-Nrp1^{A}

Confocal images of mouse mesenteries stained with antibodies against SMA (red) and Itgα9 (green). **A** and **B**, Note absence of anti-SMA staining in anti–Itgα9-positive lymphatic valves (**arrows**) in P4 wild-type mice. **C** and **D**, *Sema3a*$^{-/-}$ littermates show SMA-positive valve areas (**arrows**). **E** and **F**, Wild-type mice injected intraperitoneally with anti-Nrp1^{A}, which blocks Sema3A binding to Nrp1, exhibit SMA-positive lymphatic valves (**arrows**). **G** and **H**, SMA-positive valves are not seen after injection of anti-Nrp1^{B} (**arrows**), which blocks VEGF binding to Nrp1. **I**, Quantification of valve smooth muscle cell coverage. Itgα9-positive valve area covered by SMA-positive staining was measured. Note increase in SMC coverage of *Sema3a*$^{-/-}$ mice and Nrp1^{A}-injected mice compared with wild-type or PBS-injected counterparts. Quantification was performed using ImageJ (*P<0.05); n>4 mice per genotype. Scale bars: 20 μm.